AIMS Materials Science, 3(3): 1177-1198.
DOI: 10.3934/matersci.2016.3.1177
Received: 30 June 2016
Accepted: 10 August 2016
Published: 15 August 2016

http://www.aimspress.com/journal/Materials

Research article

Thermal degradation and crystallization characteristics of multiphase polymer systems with and without compatibilizer

Seno Jose [1,*], Jyotishkumar Parameswaranpillai [2], Bejoy Francis [3], Abi Santhosh Aprem [4], and Sabu Thomas [5]

[1] Department of Chemistry, Government College Kottayam, Kerala, India-686013
[2] Department of Polymer Science and Rubber Technology, Cochin University of Science and Technology, Cochin, Kerala, India-682022
[3] Research and Postgraduate Department of Chemistry, St. Berchmans College, Changanassery, Kottayam, Kerala, India-686101
[4] Corporate Research and Development Centre, HLL Lifecare Ltd., Akkulam, Sreekariyam P.O., Thiruvananthapuram, Kerala, India-695017
[5] Centre for Nanoscience and Nanotechnology, School of Chemical Sciences, Mahatma Gandhi University, Priyadarshini Hills P.O., Kottayam, Kerala, India-686560

* **Correspondence:** Email: senojose@gckottayam.ac.in.

Abstract: Effects of blend composition and compatibilizer concentration on the thermal degradation and crystallization characteristics of polyolefin blends are reported. Phase morphology and therefore, blend composition played a crucial role in the thermal degradation behaviour of the blends. Although compatibilization significantly improved the thermal stability of the blends, melting and crystallization parameters of the polymers were only marginally affected. Compatibilized blends with co-continuous morphology exhibited a type of "co-degradation" and "co-crystallization".

Keywords: compatibilization; thermal degradation; crystallization behaviour; co-degradation; co-crystallization

1. Introduction

Thermal degradation and crystallization characteristics of polymer blends are very relevant to the potential use of them in many applications. Thermal degradation properties are important because thermal stability of polymeric materials is one of the principal criteria for designing these materials for demanding applications [1]. Fabrication and design of a variety of articles with improved thermo-mechanical properties require a comprehensive understanding of the degradation behaviour of polymers, because the threshold temperature for degradation decides the upper limit of the fabrication temperature. It is unequivocally established that polymer blending has great impact on the thermal stability of polymer blends [2–9]. Compatibility between the components in a polymer blend is one of the decisive factors, which regulates the thermal stability of polymer blends. Moreover, it has been reported that compatibilization has profound influence on the thermal stability of multi-phase polymer systems [10–16].

Several researchers have shown that blending of polymers has significant effect on the crystallization characteristics of component polymers [17–25]. Incorporation of a second polymer into a semi-crystalline polymer may lead to (a) no change in the crystallization process [26,27,28] (b) retardation of crystallization rate [29,30] or (c) suppression or inhibition of crystallization [31,32], depending on the nature of the second component and crystallization conditions. Although a compatibilizer has a remarkable influence on the morphology of the blends, it may or may not affect the melting and crystallization characteristics [13,29,33,34,35]. Some researchers reported that incorporation of compatibilizer influences the melting and crystallization parameters of semi-crystalline polymers [29,36–41]. However, other studies have shown that unless a compatibilizer imparts molecular level miscibility, crystallization process will not be affected [13,18].

In this paper, we investigate the effect of blend composition and compatibilization on the thermal degradation characteristics and crystallization behaviour of polypropylene/high density polyethylene (PP/HDPE) blends. Thermal stability and degradation properties have been analysed by thermogravimetric method. Differential scanning calorimetry (DSC) has been employed to determine the crystallization behaviour of the blends. The activation energy for degradation was computed using Horowitz-Metzger equation. Attempt has also been made to correlate thermal degradation and crystallization characteristics of the blends with their morphology and phase structure.

2. Materials and Method

2.1. Materials

Isotactic polypropylene, PP-Koylene 3060, (MFI of 3 gram per 10 min and density of 905 kgm^{-3}) was obtained from Indian Petro Chemicals Limited, Baroda, Gujarat, India. High density polyethylene (HDPE-Relene, M60 200), having an MFI of 20 gram per 10 min and density of 960 kgm^{-3}, was supplied by Reliance Industries, India. The compatibilizer, ethylene propylene diene terpolymer (EPDM), with monomer ratio of approximately 0.5, was obtained from Herdillia Unimers Ltd., Mumbai, India.

2.2. Blend Preparation

Various compositions of PP/HDPE blends were prepared by melt-mixing at 175 °C, in a Brabender Plasticorder. The rotor speed and mixing time were optimised as 60 rev·min^{-1} and 5 min, respectively. Table 1 gives the coding system used to represent various uncompatibilized blends. Compatibilized blends were prepared by two-step mixing. First, the compatibilizer was pre-mixed with the minor component and melted for two min at 175 °C. It was followed by the addition of the major component and mixing was continued for another 5 min, at a speed of 60 rev·min^{-1} at 175 °C. For compatibilized blends, each code contains three parts: first refers to the blend, second to the compatibilizer and the third part indicates the concentration of compatibilizer in the blend with respect to the minor phase. For example, in H_{20}0.5E1, H_{20} refers to the blend composition (here 80 wt% PP and 20 wt% HDPE), 0.5E denotes the EPDM (0.5 indicates that E/P ratio is approximately 50:50) and 1 denotes the concentration of EPDM. The melt-mixed samples were compression-moulded at 185 °C to obtain sheets of 2 mm thickness.

Table 1. The coding system of uncompatibilized PP/HDPE blends.

Blend	HDPE (wt%)	PP (wt%)
H_0	0	100
H_{10}	10	90
H_{20}	20	80
H_{30}	30	70
H_{40}	40	60
H_{50}	50	50
H_{60}	60	40
H_{70}	70	30
H_{80}	80	20
H_{90}	90	10
H_{100}	100	0

2.3. Phase Morphology Studies

The morphology of cryogenically fractured surface of the blends was analysed using a Jeol Scanning Electron Microscope (SEM; Jeol 5400, Tokyo, Japan). Before analysis, the samples were sputter-coated with gold.

2.4. Thermogravimetric Analysis

The thermal degradation studies of the blends were done in a Mettler TG 50. The samples of mass approximately 10 mg were scanned from 25 °C to 600 °C at a heating rate of 20 K/min. From the TG curves, thermal degradation characteristics such as onset of degradation (T_{on}), temperature at maximum rate of degradation (T_{max}), temperatures at different weight losses and integral procedural

decomposition temperature (IPDT) have been calculated. Activation energy for degradation (E_a) was calculated using Horowitz-Metzger (HM) equation.

2.5. Differential Scanning Calorimetry

The melting and crystallization characteristics of the blends were determined using a Mettler 820 DSC thermal analyser. The mass of the sample taken for the measurement was approximately 10 mg. The first heating was done from 25 °C to 200 °C at a rate of 40 K/min, followed by isothermal heating for 3 min. The first cooling and second heating were performed at 10 K/min, in nitrogen atmosphere. The melting and crystallization characteristics were determined from the DSC heating and cooling curves, respectively. Crystallization temperature (T_c), melting point (T_m), normalised enthalpy of crystallization (ΔH_c), normalised enthalpy of fusion (ΔH_f) and percentage crystallinity ($X\%$) have been computed. The normalised values have been calculated with respect to the weight fraction of the corresponding component. The $X\%$ was estimated from the ΔH_f, using the following equation:

$$X\% = \left(\frac{\Delta H_f, norm}{\Delta H_{f100}} \right) \times 100 \tag{1}$$

where ΔH_{f100} is the enthalpy of fusion of 100% crystalline polymer. ΔH_{f100} of PP and HDPE was taken as 209 and 290 J/g, respectively.

3. Results and Discussion

3.1. Thermal Degradation Properties

3.1.1. Uncompatibilized Blends

The effect of blend composition on the thermograms (TG) and derivative thermograms (DTG) of PP/HDPE blends is given in Figure 1. A detailed evaluation of the thermograms is presented in Table 2, which gives an idea about the effect of blend composition on the temperature corresponding to different weight losses (viz. T_{on}—onset of degradation, T_{10}—temperature corresponds to 10 wt% degradation, and so on), T_{max} and IPDT. It is seen from the table that PP is more susceptible to degradation whereas HDPE shows maximum thermal stability. The T_{on} of PP (286 °C) is much lower than that of HDPE (345 °C). Thermal stability of the blends lies in between these limits. As the amount of HDPE in the blends increases, thermal stability increases. For example, the T_{on} of PP increases from 286 to 297 °C by the addition of 20 wt% of HDPE (H_{20}). However, it is important to point out that up to 50% addition of HDPE into PP (H_{50}), T_{on} increases by ca. 19 °C and further addition of 30 wt% of HDPE into PP (H_{80}) increases the T_{on} by ca. 30 °C. (The same trend is seen in the case of T_{10}, T_{20}, etc.). This implies that phase morphology (Figure 2) has a decisive role in determining the thermal stability of the blends. It should be noted that in H_{20} blend, PP is the matrix

while in H_{50} blend, both PP and HDPE form continuous phases. Thus in H_{20} and H_{50} blends, PP phase is more exposed to thermal degradation. On the other hand, in H_{80} blend, HDPE forms the matrix whereas PP the dispersed phase. As a result, HDPE matrix provides a certain level of protection to the dispersed PP phase.

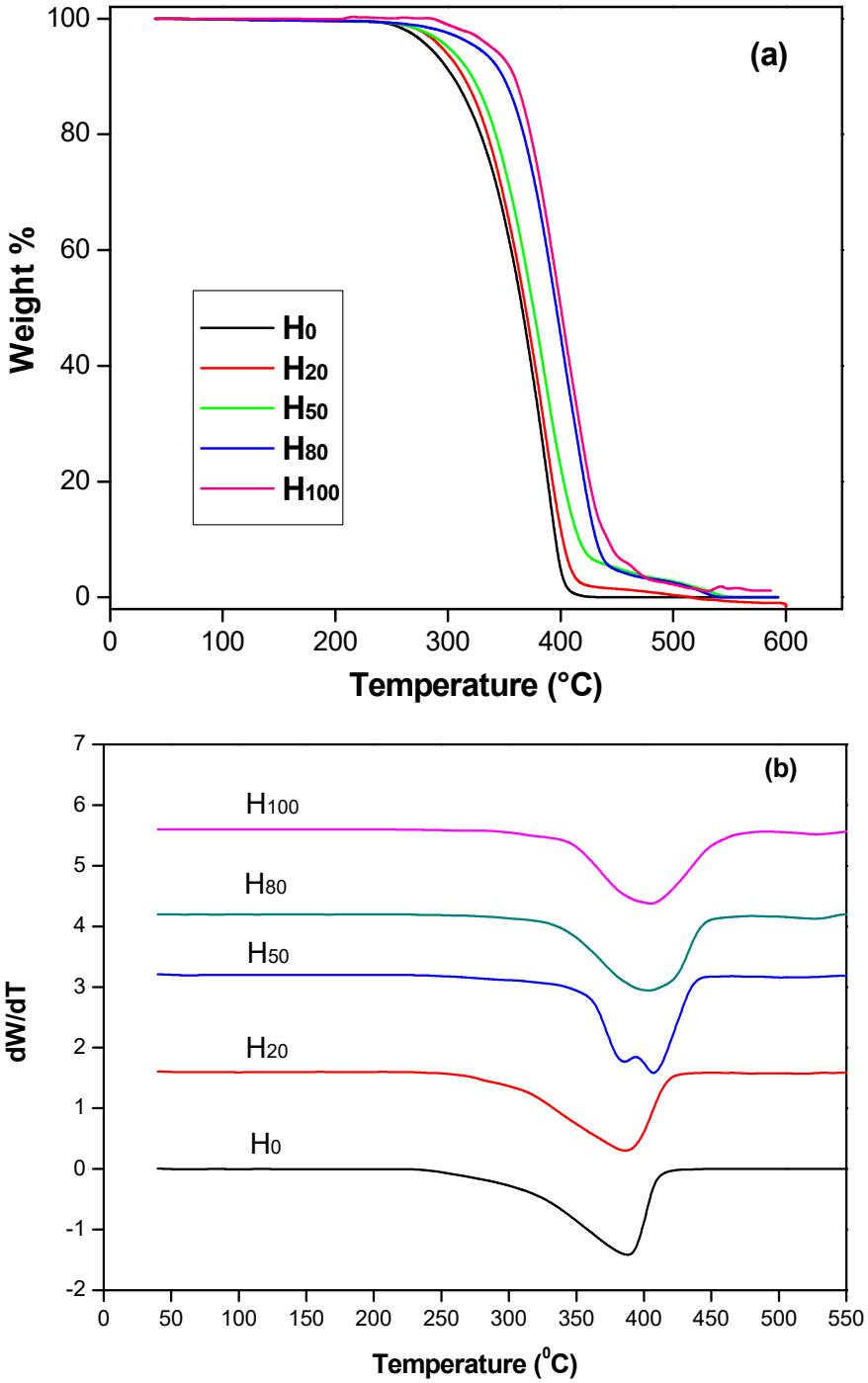

Figure 1. Effect of blend composition on the thermograms of uncompatibilized PP/HDPE blends: (a) TG and (b) DTG.

Table 2. Effect of blend composition on the temperatures corresponding to different percentage weight losses, T_{max} and IPDT of uncompatibilized PP/HDPE blends.

Blends	T_{on} (°C)	T_{10} (°C)	T_{20} (°C)	T_{30} (°C)	T_{40} (°C)	T_{50} (°C)	T_{max} (°C)	IPDT (°C)
H_0	286	307	328	345	356	365	388	356
H_{20}	297	314	334	347	360	370	387	362
H_{50}	305	322	338	353	364	376	390	374
H_{80}	335	350	367	378	386	395	407	397
H_{100}	345	356	373	384	393	401	408	406

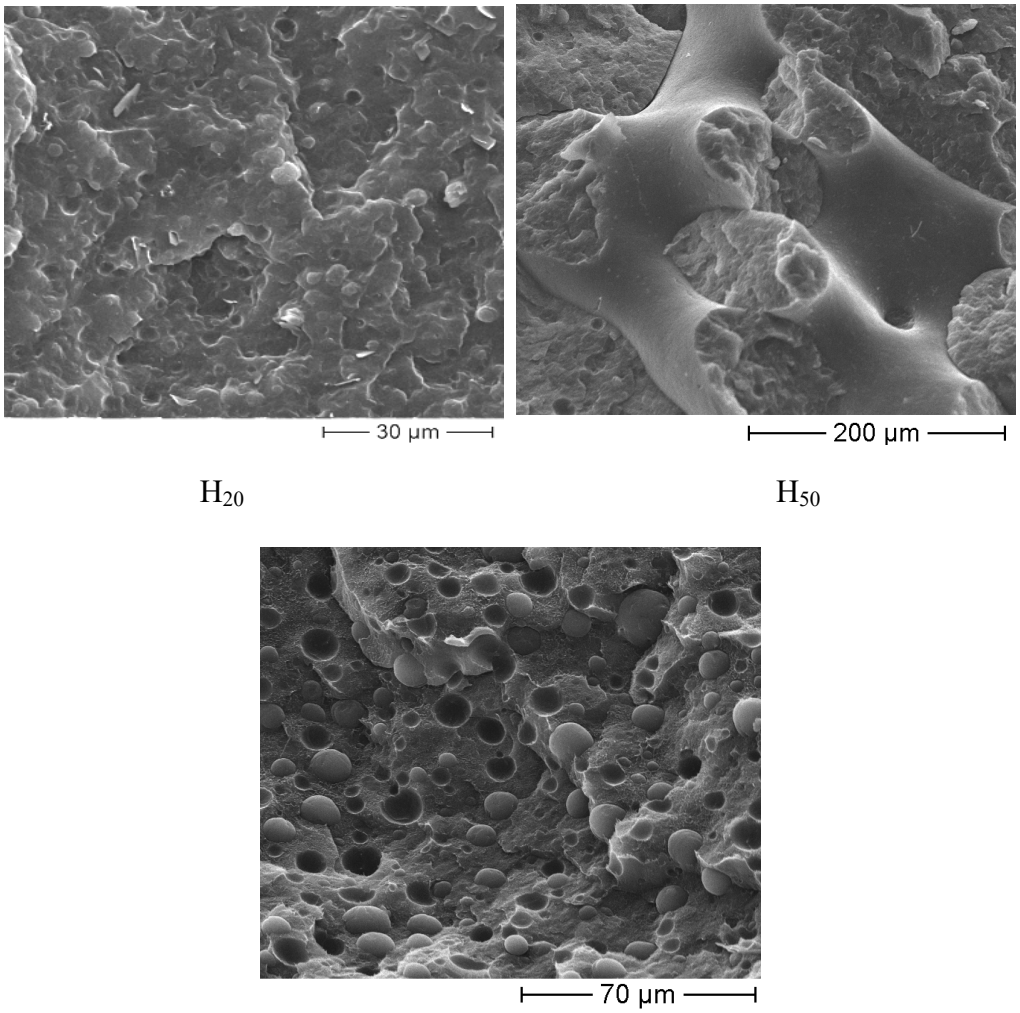

H_{20} H_{50}

H_{80}

Figure 2. SEM micrographs showing the morphology of uncompatibilized PP/HDPE blends.

IPDT has been employed to assess the relative thermal stability of blends under the procedural conditions. IPDT of the blends was measured using Doyle's method [42] given as:

$$IPDT = A^* K^* \left(T_f - T_i\right) - Ti \tag{2}$$

where T_i and T_f are the initial and final experimental temperatures, A^* is the ratio of area under the curve and the total area of the thermogram and K^* is the coefficient of A^*. Note that there is big difference between the T_{max} and IPDT of PP (ca. 32 °C) whereas the difference is negligible for HDPE (ca. 2 °C). As the amount of HDPE in the blend increases, the difference between T_{max} and IPDT decreases. Even though both T_{max} and IPDT give similar information, both are derived in different ways and in the case of completely degradable polymer systems, IPDT is more dependable since it is derived from systematic calculations. An increase in the value of T_{max} and IPDT indicates improvement in thermal stability. It is obvious from the table that as the amount of HDPE in the blend increases, thermal stability increases. A clear picture is obtained from IPDT, which shows a regular trend. Similarly, the extent of increase of both T_{max} and IPDT is different. It is also important to note that a correlation can be made between these parameters and morphology. Note that up to 50 wt% addition of HDPE into PP (H_{50}), increase in T_{max} (2 °C) and IPDT (18 °C) is not very significant, but beyond that there is considerable increase in both the parameters. For example, if the amount of HDPE in the blend increases from 50 wt% (H_{50}) to 80 wt% (H_{80}), T_{max} increases by 17 °C whereas IPDT shows an increase of 23 °C. This gives a clear indication of phase inversion. In essence, addition of HDPE into PP increases the thermal stability of the blends. In addition, thermal stability of the blends depends on the phase morphology. Moreover, the extent of improvement in thermal stability depends on the nature of morphology.

3.1.2. Compatibilized Blends

Effect of compatibilization on the thermal stability of PP/HDPE blends can be derived from the TG and DTG curves given in Figures 3 and 4. The data derived from the figures are depicted in Tables 3 and 4. Table 3 displays the effect of compatibilization on the thermal stability of H_{20} blends and Table 4 that of H_{50} blends. It is seen from the tables that compatibilization has remarkable impact on the thermal stability of the blends. For example, with the addition of 10 wt% of the compatibilizer, the T_{on} of H_{20} blend increases by ca. 13 °C whereas that of H_{50} blend by ca. 12 °C. A similar observation is seen in all cases. The T_{max} and IPDT provide same idea. In the presence of 10 wt% of compatibilizer, T_{max} of H_{20} blend increases by 15 °C and IPDT increases by 13 °C. On the other hand, for H_{50} blend, there is only marginal increase in T_{max} (4 °C). This does not imply that there is no compatibilizing action. This is basically because H_{50} blends show two degradation peaks in the absence of compatibilizer (Figure 4b), corresponding to the degradation of PP and HDPE. It is worth noting that with the addition of compatibilizer, the peaks merge together to give a single one. This occurs when the concentration of compatibilizer is only 3 wt%. The merging of peaks may be considered as a type of "co-degradation". Furthermore, it can be taken as an implication of compatibilizing action. But it is worth emphasizing that when the peaks merge together, the resultant peak is shifted towards the T_{max} of PP. This is the reason why there is no significant increase in the T_{max} of H_{50}, in the presence of compatibilizer. On the other hand, IPDT shows an increase of 13 °C. In summary, addition of compatibilizer has profound positive impact on the thermal stability of the blends. The improvement in thermal stability is mainly due to: (a) improvement in the interfacial adhesion between the components in the blends (b) reduction in the interfacial tension (c) regulation of the rate of coalescence and (d) stabilisation of the phase morphology of the blends [15,17,34].

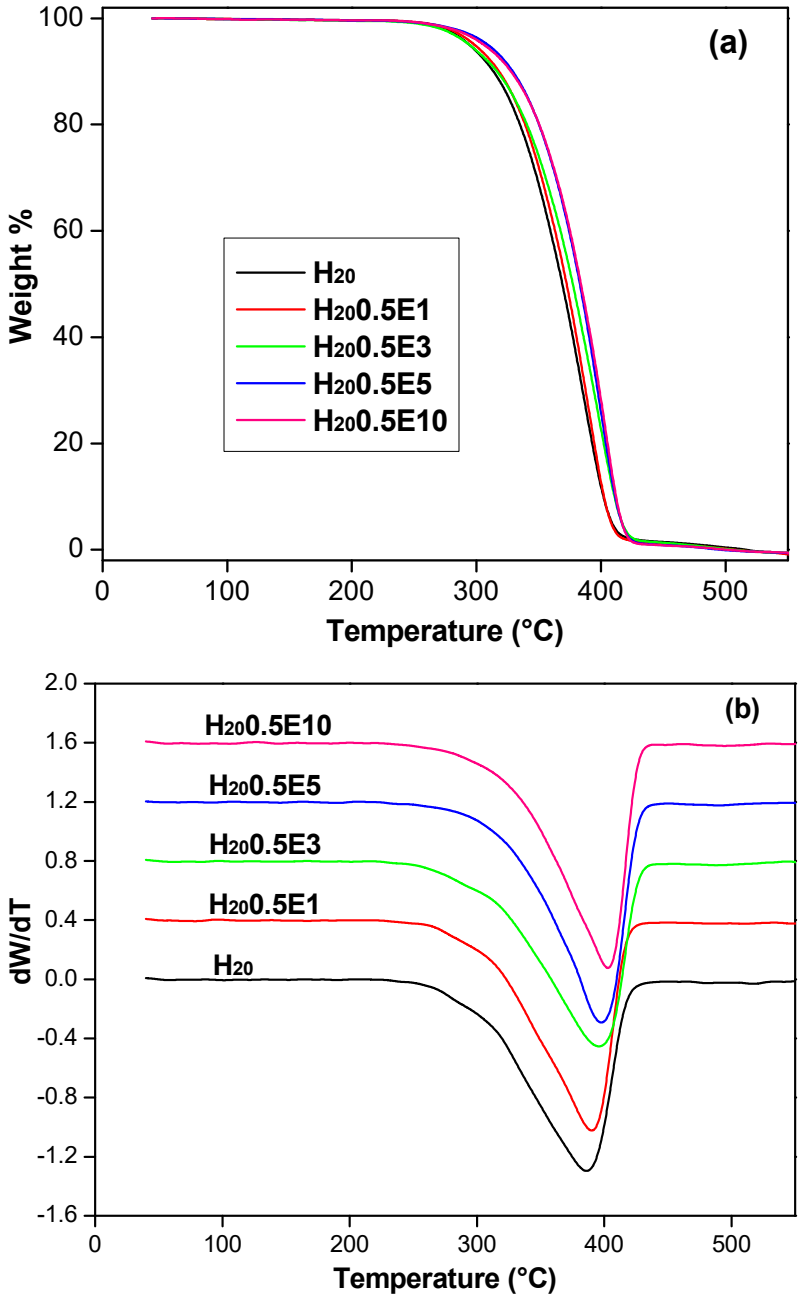

Figure 3. Effect of compatibilization on the thermograms of H_{20} blends: (a) TG and (b) DTG.

Table 3. Effect of compatibilization on the temperatures corresponding to different percentage weight losses, T_{max} and IPDT of H_{20} blends.

Blends	T_{on} (°C)	T_{10} (°C)	T_{20} (°C)	T_{30} (°C)	T_{40} (°C)	T_{50} (°C)	T_{max} (°C)	IPDT (°C)
H_{20}	297	314	334	347	360	370	386	362
H_{20}0.5E1	300	317	336	354	364	371	388	363
H_{20}0.5E3	302	318	341	358	369	378	395	372
H_{20}0.5E5	308	328	351	364	375	383	398	374
H_{20}0.5E10	310	327	349	364	373	382	401	375

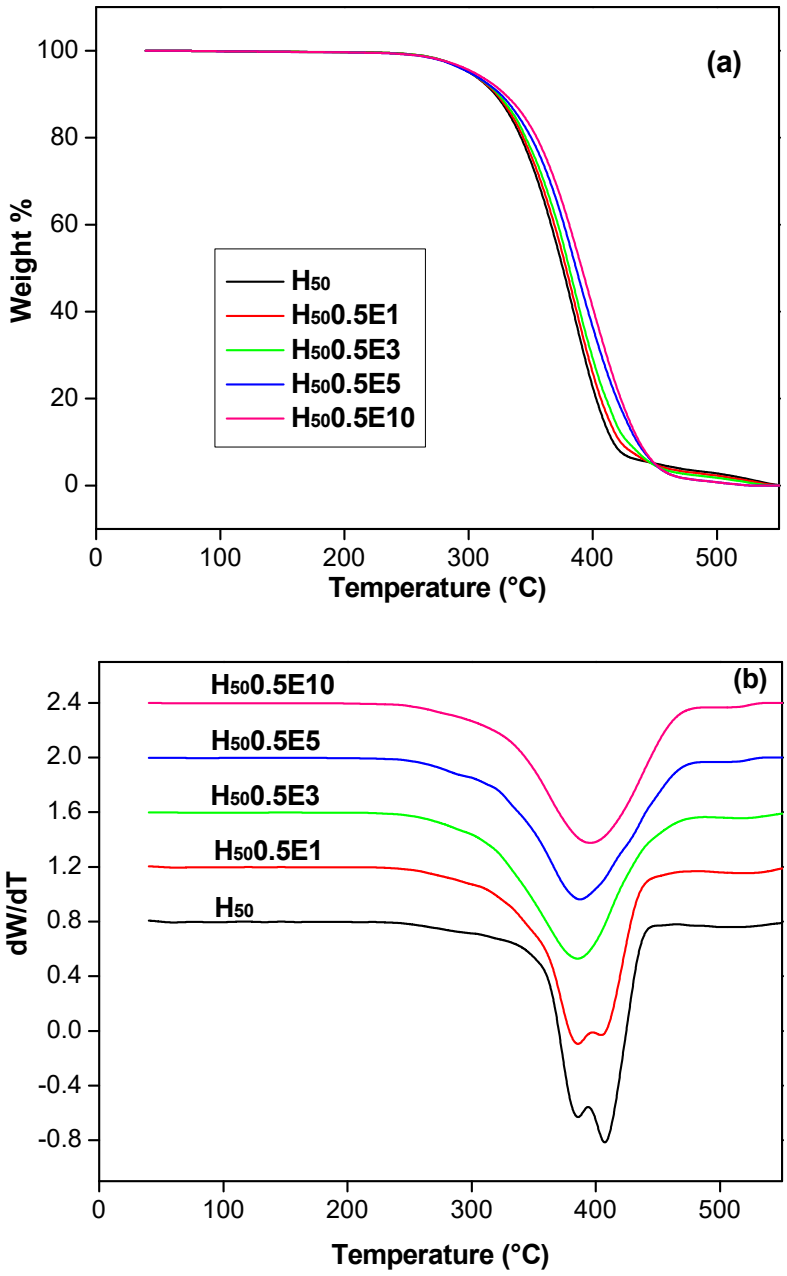

Figure 4. Effect of compatibilization on the thermograms of H_{50} blends: (a) TG and (b) DTG.

Table 4. Effect of compatibilization on the temperatures corresponding to different percentage weight losses, T_{max} and IPDT of H_{50} blends.

Blends	T_{on} (°C)	T_{10} (°C)	T_{20} (°C)	T_{30} (°C)	T_{40} (°C)	T_{50} (°C)	T_{max} (°C)	IPDT (°C)
H_{50}	305	322	338	353	364	376	390	374
H_{50}0.5E1	307	322	341	358	370	378	390	375
H_{50}0.5E3	310	324	343	360	373	380	388	378
H_{50}0.5E5	314	328	349	364	377	386	389	382
H_{50}0.5E10	317	329	353	370	379	390	394	387

Effect of compatibilizer on the matrix/droplet morphology of H_{20} blend can easily be evaluated from the SEM micrograph given in Figure 5a, because there is significant decrease in dispersed particle size. The effect of compatibilizer on the co-continuous morphology of H_{50} blend can be evaluated by comparing the SEM micrographs of annealed samples (annealed for 60 min at 180 °C) shown in Figures 5b and 5c. Morphologies of uncompatibilized and compatibilized H_{50} blends are quite different after annealing. It is important to note that the co-continuous morphology of uncompatibilized H_{50} blend is unstable and is partially converted to matrix/droplet morphology on annealing. On the other hand, H_{50} with 3 wt% compatibilizer exhibits morphological stability as there is no change in the co-continuous phase structure on annealing.

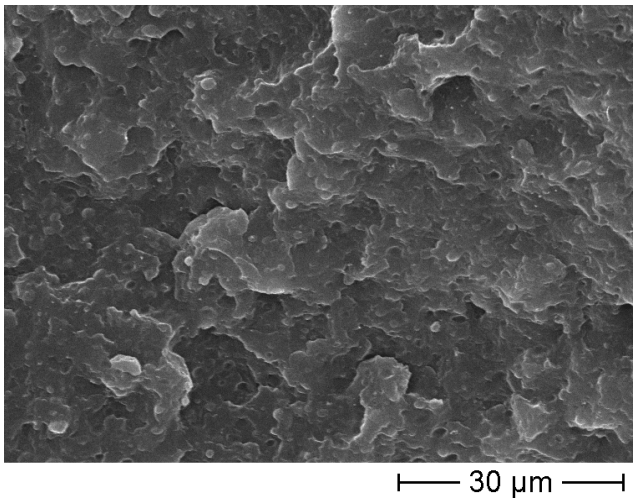

(a)

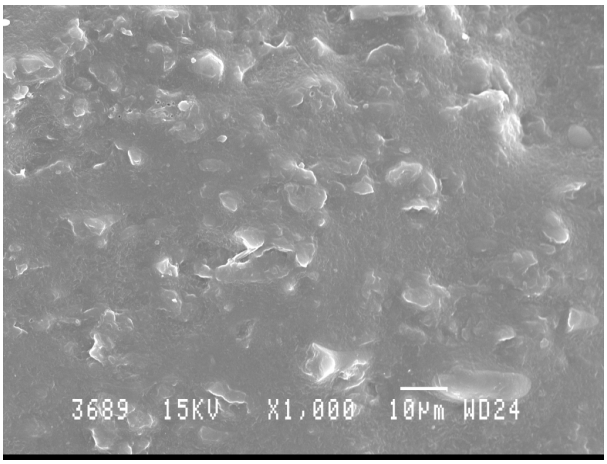

(b)

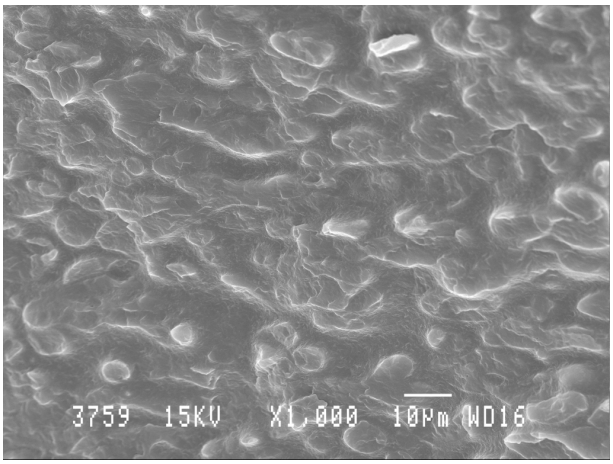

(c)

Figure 5. SEM micrographs showing the morphology of (a) H_{20} blend compatibilized with 3 wt% of compatibilizer, (b) annealed uncompatibilized H_{50} blend, (c) annealed H_{50} blend compatibilized with 3 wt% of compatibilizer.

It is well known that a compatibilizer improves the interfacial adhesion and facilitates the property transfer between the components [43]. This forces the polymer which degrades at a lower temperature to degrade at a relatively high temperature. However, the polymer which degrades at a higher temperature tends to degrade at a relatively low temperature. In effect, the presence of compatibilizer impels the degradation temperatures of the component polymers to come closer and increases the thermal stability of the blend. Note that the thermal stability of a multiphase polymer blend depends mainly on the thermal stability of the component which degrades at lower temperature. Thus, if the degradation temperatures of the individual polymers are nearer to each other, as in the case of PP and HDPE, there will be a type of "co-degradation" in the presence of compatibilizer, as observed in H_{50} blends.

3.1.3. Activation Energy for Thermal Decomposition

Activation energy for the decomposition of PP and HDPE in both uncompatibilized and compatibilized PP/HDPE blends was determined using Horowitz and Metzger (HM) method [44]. In HM method, activation energy was calculated using the equation:

$$\ln\left[\ln\left(1-\alpha\right)^{-1}\right] = E_a\left[E_a\theta/RT_{\max}^2\right] \tag{3}$$

where α is the decomposed fraction and is given as $\alpha = C_i - C/C_i - C_f$, where C is the weight at temperature chosen, C_i is the weight at initial temperature and C_f is the weight at final temperature, E_a is the activation energy for decomposition, R is the universal gas constant and θ is given by $T - T_{max}$. Kinetic plots were made with $\ln\left[\ln\left(1-\alpha\right)^{-1}\right]$ versus θ. From the slope of the plots, E_a was calculated.

Figure 6 shows the Arrhenius plots for the activation energy for the decomposition (E_a) of PP and HDPE, in uncompatibilized PP/HDPE blends. The effects of blend composition and compatiblization on the E_a of PP and HDPE are given in Table 5. E_a of PP and HDPE are 118.3 and 145.3 kJ/mol, respectively. It is seen that addition of HDPE into PP increases the E_a of the blends. Although the blends are heterogeneous, only one E_a is reported for each blend. This is because it was difficult to resolve the degradation peaks of PP and HDPE in the blends into two, as there was no big difference in the temperatures for major degradation of PP and HDPE. In fact, two maxima were observed for H_{50} blend. Since the peaks were very close to each other, we considered the peaks as a single peak to avoid the complexity in calculating the E_a. This is the reason why H_{50} blend exhibits relatively lower E_a than expected. It is also important to note that an increase in E_a implies an improvement in thermal stability of the blends. Thus, it can be concluded that as the amount of HDPE in the blend increases, the thermal stability also increases.

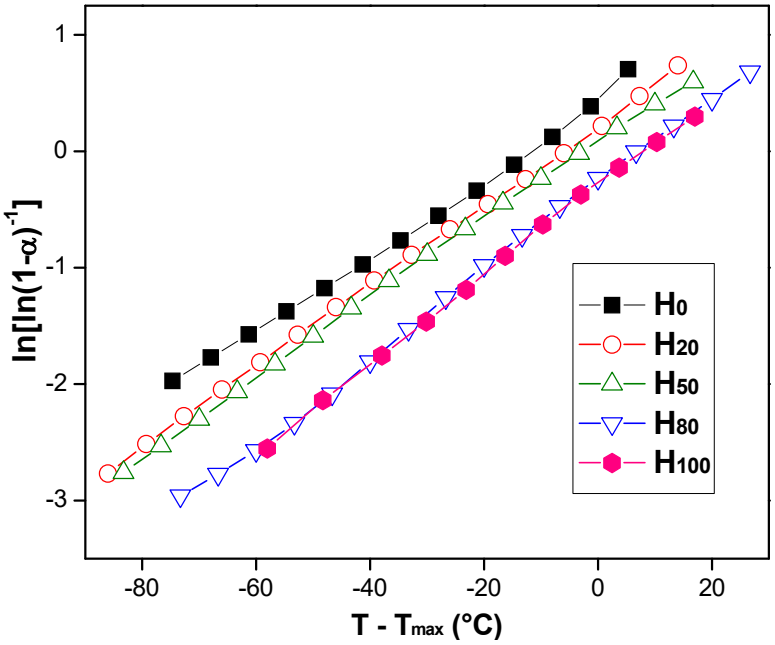

Figure 6. Arrhenius plots for calculating the activation energy for degradation of PP, HDPE and their blends.

Table 5. Effect of blend composition and compatibilization on the activation energy for degradation of PP/HDPE blends.

Blends	E_a (kJ/mol)	Blends	E_a (kJ/mol)	Blends	E_a (kJ/mol)
H_0	118.3	H_{20}	124.2	H_{50}	123.8
H_{20}	124.2	H_{20}0.5E1	127	H_{50}0.5E1	120.4
H_{50}	123.8	H_{20}0.5E3	132.3	H_{50}0.5E3	115
H_{80}	141.6	H_{20}0.5E5	137.4	H_{50}0.5E5	109
H_{100}	145.3	H_{20}0.5E10	134.3	H_{50}0.5E10	109

The effect of compatibilization on the Arrhenius plots for calculating the E_a for degradation of H_{20} blends is displayed in Figure 7a. It is obvious from table that addition of compatibilizer improves the E_a of H_{20} blends. This means that as the amount of compatibilizer increases, the tendency to undergo thermal decomposition decreases indicating improved thermal stability. However, in the presence of 10 wt% of compatibilizer, E_a slightly decreases. On the other hand, interestingly, E_a of H_{50} blends decreases in the presence of compatibilizer (Figure 7b). This is quite unexpected. However, attention should be paid to the fact that the degradation peaks of PP and HDPE merge together, in the presence of compatibilizer. This indicates that the degradation of both PP and HDPE occur simultaneously. From Figure 4b, it is clear that the degradation peak of the blend is shifted to the temperature corresponds to the degradation of PP (which has a lower E_a) indicating a type of "co-degradation".

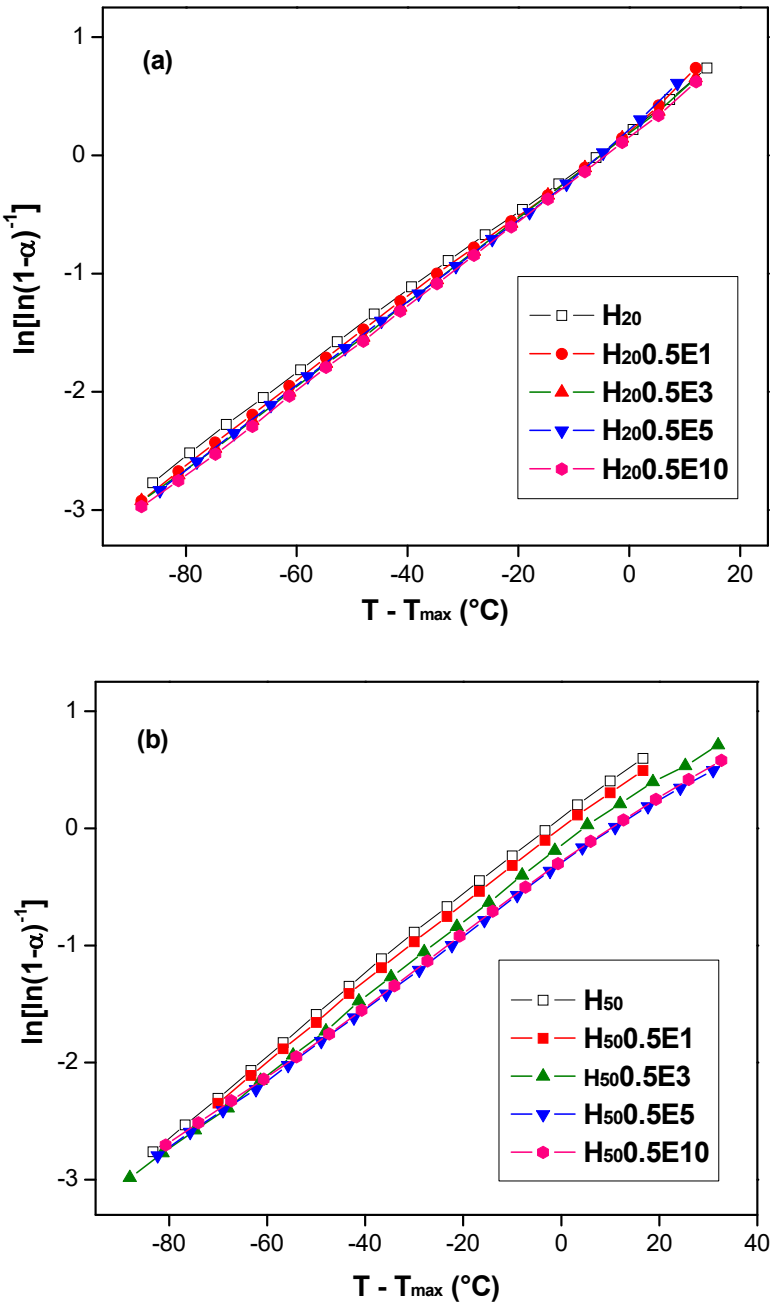

Figure 7. Effect of compatibilization on the Arrhenius plots for calculating the activation energy for degradation of PP/HDPE blends: (a) H_{20} and (b) H_{50}.

3.2. Melting and Crystallization Behaviour

3.2.1. Uncompatibilized Blends

It has been reported that the type of morphology and therefore blend composition has a crucial role in the crystallization behaviour of polymer blends [29,45–49]. Table 6 shows the effect of blend ratio on the T_c, T_m and the normalised values of ΔH_c and ΔH_f of PP and HDPE.

Table 6. Effect of blend composition on the crystallization temperature (T_c), melting temperature (T_m), normalised values of enthalpies of crystallization (ΔH_c) and fusion (ΔH_f) of PP and HDPE in uncompatibilized PP/HDPE blends.

Blends	T_c (°C)		T_m (°C)		ΔH_c (J/g)		ΔH_f (J/g)	
	PP	PE	PP	PE	PP	PE	PP	PE
H_0	126	---	165	---	96	---	94	---
H_{10}	128	118	166	131	98	177	96	175
H_{20}	128	117	166	130	94	185	91	179
H_{30}	127	118	165	132	95	179	96	181
H_{40}	127	119	166	131	99	178	95	179
H_{50}	126	118	165	132	94	182	97	178
H_{60}	125	117	164	130	95	181	93	180
H_{70}	126	118	164	133	93	185	90	178
H_{80}	125	117	163	133	92	185	90	183
H_{90}	125	117	163	130	83	187	81	186
H_{100}	---	117	---	132	--	184	--	180

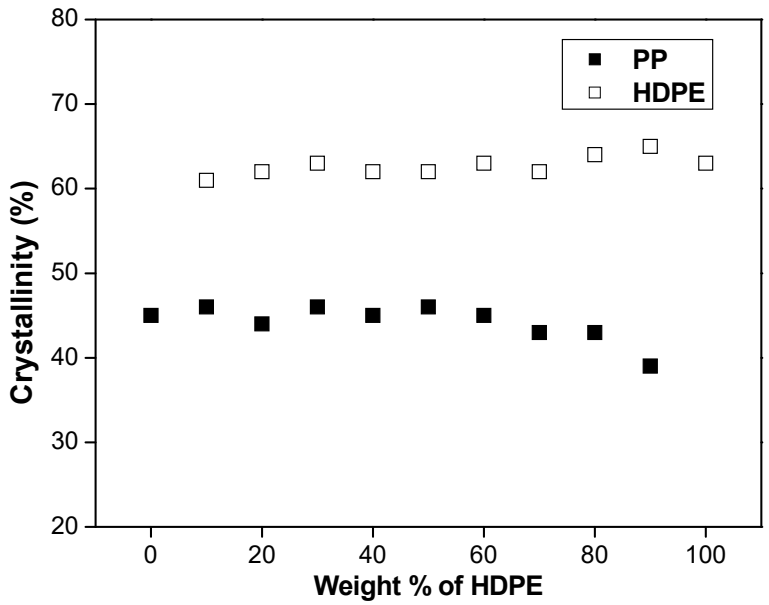

Figure 8. Effect of blend composition on the percentage crystallinity of HDPE and PP in PP/HDPE blends.

The T_c of PP and HDPE are found to be 126 and 117 °C, respectively, whereas T_m of PP and HDPE are observed as 165 and 132 °C, respectively. It is seen that blend composition has no appreciable effect on the T_c and T_m of component polymers. This is not unexpected since PP/HDPE blends are immiscible and incompatible. As a result, the crystallization characteristics of individual components are little affected. It is observed from the table that ΔH_c and ΔH_f of PP are considerably less than that of HDPE. The percentage crystallinity of PP and HDPE is presented in Figure 8. The

crystallinity of PE (ca. 62%) is greater than that of PP (ca. 45%). At the same time, it is important to note that there is no considerable change in the % crystallinity of components in their blends. In summary, the melting and crystallization characteristics of PP/HDPE blends reveal that blend composition has little impact on these properties due to the lack of specific interactions between the components signifying the immiscible nature of the blends.

3.2.2. Compatibilized Blends

The melting and crystallization characteristics of compatibilized H_{20} blends are summarised in Table 7.

Table 7. Effect of compatibilization on the crystallization temperature (T_c), melting temperature (T_m), normalised values of enthalpies of crystallization (ΔH_c) and fusion (ΔH_f) of PP and HDPE in H_{20} blends.

Blends	T_c (°C)		T_m (°C)		ΔH_c (J/g)		ΔH_f (J/g)	
	PP	PE	PP	PE	PP	PE	PP	PE
H_{20}	128	117	166	130	94	185	91	179
H_{20}0.5E1	128	117	167	130	95	183	92	178
H_{20}0.5E3	128	116	167	131	93	179	91	179
H_{20}0.5E5	127	117	166	130	91	180	92	179
H_{20}0.5E10	128	117	165	130	92	181	93	178

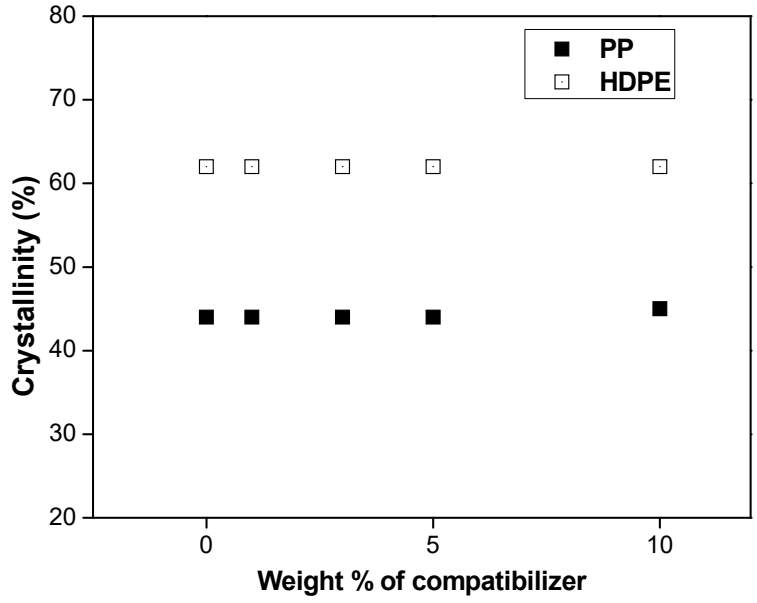

Figure 9. Effect of compatibilization on the percentage crystallinity of PP and HDPE in H_{20} blends.

It is obvious from the table that incorporation of compatibilizer has no appreciable effect on the T_c and T_m of PP and HDPE. This implies that compatibilizer has no significant influence on the crystallization kinetics of polymer blends. Note that compatibilizer locates at the interface between the component polymers and decreases the unfavourable cross-correlations between them or increases favourable interactions. Since the physical compatibilizer stays only at the interface between the phases, there are only physical interactions between the components. These physical interactions do not lead to any type of miscibility or chemical bonds between the components. It is also observed that the ΔH_c and ΔH_f of PP and HDPE are also not considerably affected by the presence of compatibilizer even though there is marginal decrease in ΔH_c and ΔH_f values. Similarly, the percentage crystallinity of PP and HDPE are also little affected by the addition of compatibilizer (Figure 9).

The cooling and heating curves of compatibilized H_{50} blends are shown in Figures 10a and 10b, respectively (Note that the Y—axis of the heating and cooling curves is arbitrarily taken). Although the heating curves demonstrate no effect on the melting behaviour of the blends on compatibilization, the cooling curves provide some interesting observations. The cooling curves of compatibilized blends show a type of "co-crystallization" phenomenon, in the presence of compatibilizer. Note that with increase in the amount of compatibilizer, the two crystallization peaks approach each other and at 5 wt% of the compatibilizer, the two peaks merge together leading to "co-crystallization" behaviour. This indicates that in H_{50} blend, compatibilizer has a certain level of influence on the crystallization process.

The main difference between H_{20} and H_{50} blends is that in H_{20} blends, HDPE exists as dispersed domains in PP matrix whereas in H_{50} blends, both the phases are continuous. Thus in H_{50} blends, the crystallization process of each component may be affected by the presence of the other component (in the presence of compatibilizer). Joseph et al. [48] reported that spherulite growth of PP may change when matrix/droplet morphology changes to co-continuous, since the latter may slow down the crystal growth. On the other hand, in the case of blends with matrix/droplet morphology (H_{20}), the crystallization process of the minor phase may be affected by the presence major phase. Note that PP crystallizes earlier than PE. This means that PP solidifies first so that in H_{20} blend, even if HDPE forms the dispersed phase, the crystallization process of HDPE is not affected by the presence of PP since during the crystallization process of HDPE, PP is in solid state. On the other hand, in the case of H_{50} blends, since it possesses co-continuous phase structure, the presence of HDPE phase affects the crystallization process of PP, which occurs earlier. But this happens only in the presence of the compatibilizer since in the absence of compatibilizer, the blends are highly incompatible and there is little probability for one component to interfere with the properties of the other. Thus in the presence of compatibilizer, the crystallization process of PP is suppressed by HDPE phase because PP solidifies in the vicinity of molten HDPE so that both the phases crystallize simultaneously near the T_c of HDPE (Table 8). Note that the resulting peak appears at ca. 116 °C, which is the T_c of HDPE. This means that compatibilizer suppresses the crystallization of PP phase and enables the "co-crystallization" phenomenon to occur, near the T_c of HDPE. It should be noted that in the absence of compatibilizer, two distinct crystallization peaks correspond to PP and HDPE can be obtained.

Table 8. Effect of compatibilization on the crystallization temperature (T_c), melting temperature (T_m), normalised values of enthalpies of crystallisation (ΔH_c) and fusion (ΔH_f) of PP and HDPE in H_{50} blends.

Blends	T_c (°C)		T_m (°C)		ΔH_c (J/g)		ΔH_f (J/g)	
	PP	PE	PP	PE	PP	PE	PP	PE
H_{50}	126	118	165	132	165	132	97	178
H_{50}0.5E1	124	116	166	133	166	133	90	178
H_{50}0.5E3	---	115	165	130	260		89	177
H_{50}0.5E5	---	116	165	132	258		87	175
H_{50}0.5E10	---	116	164	130	252		85	174

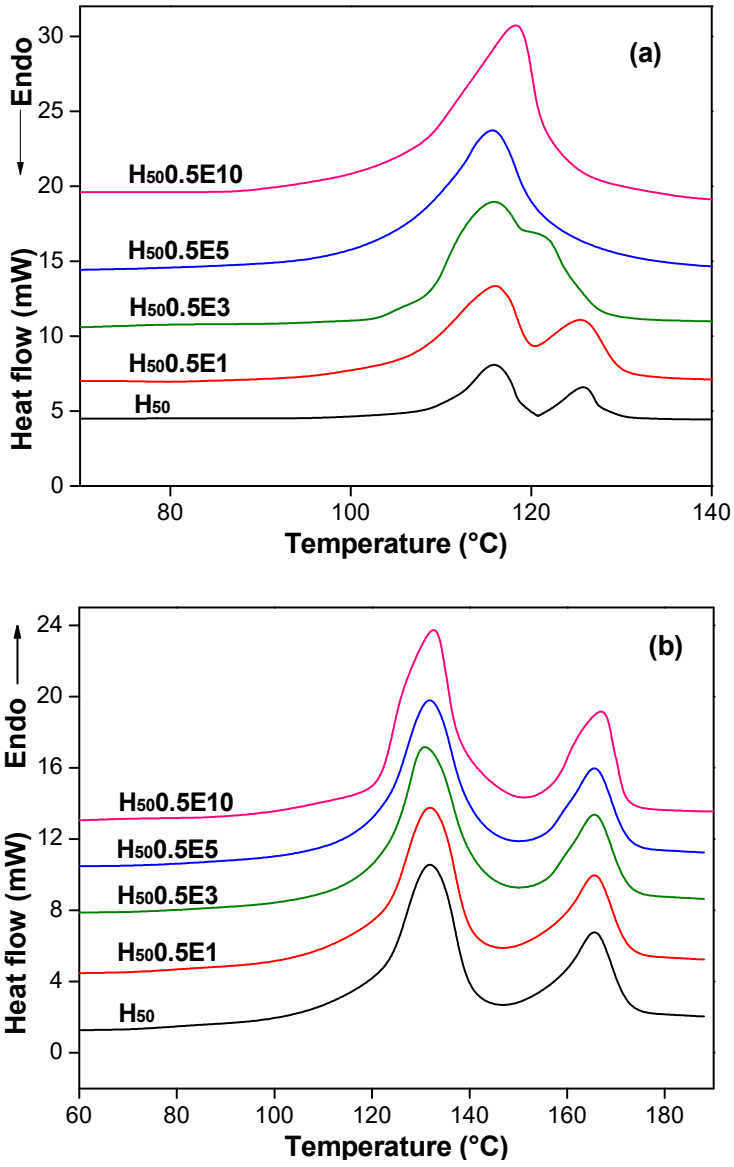

Figure 10. Effect of compatibilization on the DSC thermograms of H_{50} blends: (a) cooling curves and (b) heating curves.

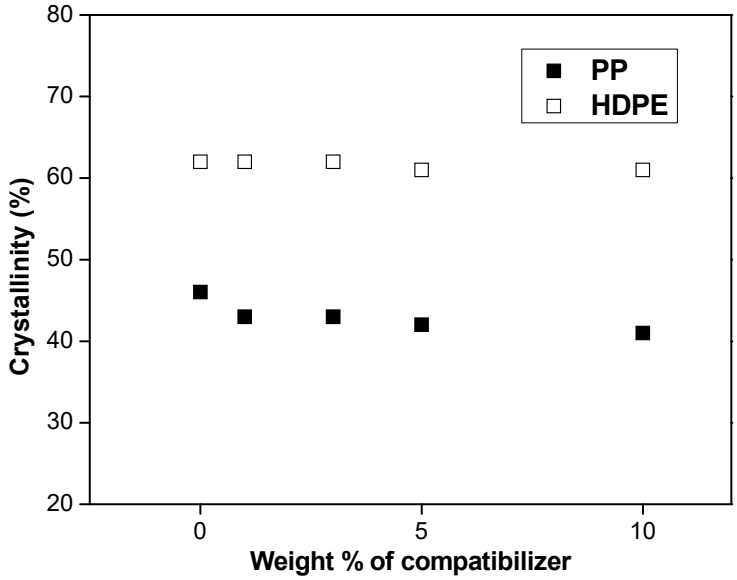

Figure 11. Effect of compatibilization on the percentage crystallinity of PP and HDPE in H_{50} blends.

Table 8 shows that the ΔH_c values calculated from the area of crystallization peak is almost equal to the sum of the ΔH_c's of neat PP and HDPE. However, note that the ΔH_f marginally decreases with increase in concentration of compatibilizer. Similar information is obtained from the Figure 11, which shows the effect of compatibilizer on the percentage crystallinity of H_{50} blends. In essence, it can be presumed that despite compatibilization has no significant role on the melting behaviour of PP/HDPE blends, under appropriate morphological conditions, crystallization process may be affected.

4. Conclusions

The present study was devoted to investigate the effect of blend composition and compatibilizer concentration on the thermal degradation and crystallization characteristics of polypropylene/high density polyethylene (PP/HDPE) blends. Addition of HDPE into PP significantly improved the thermal stability of the blends. Despite the heterogeneous nature of the blends, all the blends except PP/HDPE 50/50 blends, showed only single degradation peak. EPDM copolymer was used as the compatibilizer. The compatibilizer considerably improved the thermal stability of the blends. The activation energy for degradation of PP/HDPE blends, calculated using Horowitz Metzger equation, increased with HDPE content in the blends. However, PP/HDPE 50/50 blends showed lower activation energy than expected. It was also observed that the incorporation of compatibilizer improved the activation energy of 80/20 PP/HDPE blends. On the other hand, for PP/HDPE 50/50 blends, activation energy decreased with compatibilizer addition. Moreover, compatibilized PP/HDPE 50/50 blends displayed a type of "co-degradation" at the temperature corresponding to the maximum degradation of PP. The melting and crystallization characteristics of the blends showed that blend composition has no effect on these properties. It was also observed that compatibilization has just marginal impact on the

melting and crystallization behaviour of PP/HDPE 80/20 blends. However in PP/HDPE 50/50 blends, with the addition of compatibilizer, the crystallization peaks of PP and HDPE merged together to give a single peak. The merging took place even in the presence of 3 wt% of the compatibilizer. This was considered as a type of "co-crystallization" of the two crystalline polymers as there is no big difference in their crystallization temperatures.

Conflict of Interest

The authors declare that there is no conflict of interest regarding the publication of this manuscript.

References

1. Clough RL, Billingham NC, Gillen KT (1996) Polymer durability, degradation, stabilization and lifetime prediction, Eds. American Chemical Society, Washington DC.
2. Varghese H, Bhagavan SS, Thomas S (2001) Thermogravimetric analysis and thermal ageing of crosslinked nitrile rubber/poly(ethylene-co-vinyl acetate) blends. *J Therm Analy Calor* 63: 749–763.
3. Stephen R, Jose S, Joseph K, et al. (2006) Thermal stability and ageing properties of sulphur and gamma radiation vulcanized natural rubber (NR) and carboxylated styrene butadiene rubber (XSBR) latices and their blends. *Polym Degrad Stab* 91: 1717–1725.
4. Stephen R, Siddique AM, Singh F, et al. (2007) Thermal degradation and ageing behavior of microcomposites of natural rubber, carboxylated styrene butadiene rubber latices, and their blends. *J Appl Polym Sci* 105: 341–351.
5. Komalan C, George KE, Varughese KT, et al. (2008) Thermogravimetric and wide angle X-ray diffraction analysis of thermoplastic elastomers from nylon copolymer and EPDM rubber. *Polym Degrad Stab* 93: 2104–2112.
6. Thomas R, Yumei D, Yuelong H, et al. (2008) Miscibility, morphology, thermal, and mechanical properties of a DGEBA based epoxy resin toughened with a liquid rubber. *Polymer* 49: 278–294.
7. Johns J, Rao V (2009) Thermal stability, morphology, and X-ray diffraction studies of dynamically vulcanized natural rubber/chitosan blends. *J Mater Sci* 44: 4087–4094.
8. Singh G, Bhunia H, Rajor A, et al. (2011) Thermal properties and degradation characteristics of polylactide, linear low density polyethylene, and their blends. *Polym Bull* 66: 939–953.
9. Mofokeng JP, Luyt AS (2015) Morphology and thermal degradation studies of melt-mixed poly(lactic acid) (PLA)/poly(ε-caprolactone) (PCL) biodegradable polymer blend nanocomposites with TiO_2 as filler. *Polym Test* 45: 93–100.
10. Asaletha R, Kumaran MG, Thomas S (1998) Thermal behaviour of natural rubber/polystyrene blends: thermogravimetric and differential scanning calorimetric analysis. *Polym Degrad Stab* 61: 431–439.
11. George S, Varughese KT, Thomas S (2000) Thermal and crystallization behaviour of isotactic polypropylene/nitrile rubber blends. *Polymer* 41: 5485–5503.

12. OOmmen Z, Groeninckx G, Thomas S (2000) Dynamic mechanical and thermal properties of physically compatibilized natural rubber/poly(methyl methacrylate) blends by the addition of natural rubber-*graft*- poly(methyl methacrylate). *J Polym Sci B Polym Phys* 38: 525–536.
13. Jose S, Thomas S, Biju PK, et al. (2008) Thermal degradation and crystallization studies of reactively compatibilized polymer blends. *Polym Degrad Stab* 93: 1176–1187.
14. Borah JS, Chaki TK (2011) Thermogravimetric and dynamic mechanical analysis of LLDPE/EMA blends. *J Therm Anal Calorim* 105: 365–373.
15. Kannan M, Bhagawan SS, Thomas S, et al. (2012) Thermogravimetric analysis and differential scanning calorimetric studies on nanoclay-filled TPU/PP blends. *J Therm Anal Calorim* 112: 1231–1244.
16. Yousfi M, Livi S, Dumas A, et al. (2015) Ionic compatibilization of polypropylene/polyamide 6 blends using an ionic liquids/nanotalc filler combination: morphology, thermal and mechanical properties. *RSC Adv* 5: 46197–46205.
17. Jose S, Aprem AS, Francis B, et al. (2004) Phase morphology, crystallization behaviour and mechanical properties of isotactic polypropylene/high density polyethylene blends. *Eur Polym J* 40: 2105–2115.
18. Moly KA, Radusch HJ, Androsh R, et al. (2005) Non-isothermal crystallization, melting behaviour and wide angle X-ray scattering investigations on linear low density polyethylene (LLDPE)/ethylene vinyl acetate (EVA) blends: effects of compatibilization and dynamic crosslinking. *Eur Polym J* 41: 1410–1419.
19. Costa HMD, Ramos VD (2008) Analysis of thermal properties and rheological behavior of LLDPE/EPDM and LLDPE/EPDM/SRT mixtures. *Polym Test* 27: 27–34.
20. Chen H, Pyda M, Cebe P (2009) Non-isothermal crystallization of PET/PLA blends. *Thermochimica Acta* 492: 61–66.
21. Joseph A, Luftl S, Seidler S, et al. (2009) Non-isothermal thermophysical evaluation of polypropylene/natural rubber based TPEs: effect of blend ratio and dynamic vulcanization. *Polym Eng Sci* 49: 1332–1339.
22. Borah JS, Chaki TK (2011) Dynamic mechanical, thermal, physico-mechanical and morphological properties of LLDPE/EMA blends. *J Polym Res* 18: 569–578.
23. Buccella M, Dorigato A, Pasqualini E, et al. (2012) Thermo-mechanical properties of polyamide 6 chemically modified by chain extension with polyamide/polycarbonate blend. *J Polym Res* 19: 1–9.
24. Madi NK (2013) Thermal and mechanical properties of injection molded recycled high density polyethylene blends with virgin isotactic polypropylene. *Mater Design* 46: 435–441.
25. Chen R, Zou W, Wu C, et al. (2014) Poly(lactic acid)/poly(butylene succinate)/calcium sulphate whiskers biodegradable blends prepared by vane extruder: analysis of mechanical properties, morphology, and crystallization behaviour. *Polym Test* 34: 1–9.
26. Razavi-Nouri M, Hay JN (2006) Isothermal crystallization and spherulite nucleation in blends of polypropylene with metallocene-prepared polyethylene. *Polym Int* 55: 6–11.
27. Jose S, Thomas PS, Thomas S, et al. (2006) Thermal and crystallization behaviours of blends of polyamide 12 with styrene-ethylene/butylene-styrene rubbers. *Polymer* 47: 6328–6336.

28. Xu C, Yuan D, Fu L, et al. (2014) Physical blend of PLA/NR with co-continuous phase structure: Preparation, rheology property, mechanical properties and morphology. *Polym Test* 37: 94–101.
29. Joseph A, George S, Joseph K, et al. (2006) Melting and crystallization behaviors of isotactic polypropylene/acrylonitrile-butadiene rubber blends in the presence and absence of compatibilizers and fillers. *J Appl Polym Sci* 102: 2067–2080.
30. Svoboda P, Svobodova D, Slobodian P, et al. (2009) Crystallization kinetics of polypropylene/ethylene-octane copolymer blends. *Polym Test* 28: 215–222.
31. Aravind I, Boumod A, Grohens Y, et al. (2010) Morphology, dynamic mechanical, thermal, and crystallization behaviors of poly(trimethylene terephthalate)/polycarbonate blends. *Ind Eng Chem Res* 49: 3873–3882.
32. Xie X, Bai W, Wu A, et al. (2014) Increasing the compatibility of poly(L-lactide)/poly(para-dioxanone) blends through the addition of poly(para-dioxanone-co-L-lactide). *J Appl Polym Sci* 132.
33. Marco C, Ellis G, Gomez MA, et al. (1997) Rheological properties, crystallization, and morphology of compatibilized blends of isotactic polypropylene and polyamide. *J Appl Polym Sci* 65: 2665–2677.
34. Sato H, Katsumoto Y, Sasao S, et al. (2002) Raman, X-ray diffraction and differential scanning calorimetry studies of the melt-induced changes in uncompatibilized and compatibilized blends of high-density polyethylene and nylon 12. *Macromol Symp* 184: 339–348.
35. Dou R, Wang W, Zhou Y, et al. (2013) Effect of core-shell morphology evolution on the rheology, crystallization, and mechanical properties of PA6/EPDM-*g*-MA/HDPE ternary blend. *J Appl Polym Sci* 129: 253–262.
36. Choudhary V, Varma HS, Varma IK (1991) Polyolefin blends: effect of EPDM rubber on crystallization, morphology and mechanical properties of polypropylene/EPDM blends. *Polymer* 32: 2534–2540.
37. Lin Z, Chen C, Li B, et al. (2012) Compatibility, morphology, and crystallization behavior of compatibilized β-nucleated polypropylene/poly(trimethylene terephthalate) blends. *J Appl Polym Sci* 125: 1616–1624.
38. Zhu Y, Liang C, Bo Y, et al. (2015) Non-isothermal crystallization behavior of compatibilized polypropylene/recycled polyethylene terephthalate blends. *J Therm Anal Calorim* 119: 2005–2013.
39. Rastin H, Saeb MR, Jafari SH, et al. (2015) Reactive compatibilization of ternary polymer blends with core-shell type morphology. *Macromol Mater Engg* 300: 86–98.
40. Parameswaranpillai J, Joseph G, Jose S, et al. (2015) Phase morphology, thermomechanical, and crystallization behaviour of uncompatibilized and PP-g-MAH compatibilized polypropylene/polystyrene blends. *J Appl Polym Sci* 132.
41. Ponnamma D, George J, Thomas MG, et al. (2015) Investigation on the thermal and crystallization behavior of high density polyethylene/acrylonitrile butadiene rubber blends and their composites. *Polym Eng Sci* 55: 1203–1210.
42. Doyle CD (1961) Estimating thermal stability of experimental polymers by empirical thermogravimetric analysis. *Anal Chem* 33: 77–79.

43. Jose S, Thomas S, Biju PK, et al. (2013) Mechanical and dynamic mechanical properties of polyolefin blends: effect of blend ratio and copolymer monomer fraction on the compatibilization efficiency of random copolymers. *J Polym Res* 20: 1–13.
44. Horowitz HH, Metzger G (1963) A new analysis of thermo gravimetric traces. *Anal Chem* 35: 1464–1468.
45. Li C, Tian G, Zhang Y, et al. (2002) Crystallization behavior of polypropylene/polycarbonate blends. *Polym Test* 21: 919–926.
46. Wong CY, Lam F (2002) Study of selected thermal characteristics of polypropylene/polyethylene binary blends using DSC and TGA. *Polym Test* 21: 691–696.
47. Dangseeyun N, Supaphol P, Nithitanakul M (2004) Thermal, crystallization, and rheological characteristics of poly(trimethylene terephthalate)/poly(butylene terephthalate) blends. *Polym Test* 23: 187–194.
48. Joseph A, Koch T, Seidler S, et al. (2008) Crystallization behavior and spherulite growth rate of isotactic polypropylene in isotactic polypropylene/natural rubber based thermoplastic elastomers. *J Appl Polym Sci* 109: 1714–1721.
49. Rosa DS, Grillo D, Bardi MAG, et al. (2009) Mechanical, thermal and morphological characterization of polypropylene/biodegradable polyester blends with additives. *Polym Test* 28: 836–842.

AIMS Press